Investigation of the influence of the distance and the angle of observation in radiometric measurements in the infrared spectrum

Hristo I. Hristov[1] and Kalin L. Dimitrov[2]

Abstract – **In this study, we will outline some significant possibilities of infrared radiometry for measurements of plant surface temperature. We will consider the importance of the distance from the object to the radiometer, as well as the angle at which the radiometer registers the radiation. We will show how the change of these two factors affects the heat flux that enters the aperture of the radiometer from the object.**

Keywords – **infrared thermography, infrared radiometry, surface temperature, plants, emission coefficient, agriculture**

I. Introduction

Today, many new technologies and innovations are focused on agriculture, agribusiness, and the environment. Infrared thermography plays an important role in remote temperature measurements. It is involved in the detection and study of different types of stress in plants and plays a key role in research on temperature stress and their ability to acclimatize and survive in various severe temperature conditions [1-2]. Sensors operating in the 8-14 μm range are used for infrared imaging, as those operating in the 3-5 μm range are not suitable for daytime use due to their high sensitivity to reflected solar radiation [3]. Thermography is involved in methods for evaluating seeds as propagating material [4]. It also plays an important role in plant protection. Different pathogens can change the processes of evaporation, which changes the water balance, and hence the distribution of surface temperature. Thermography allows for early detection of infected leaves before symptoms appear in the visible spectrum [5]. Due to the impossibility of always accurately identifying the cause of a particular problem, thermography can be used in the field to locate places where the culture is more affected and therefore it is necessary to respond more quickly. It can be used to monitor the content of various nutrients in crops, thus the processes of fertilization and introduction into the soil of the substances necessary for plant development become timely and correct [6]. Infrared thermography has been successfully used to study the interactions between plants and the environment, for ecological research and natural monitoring. With the help of infrared thermography, remote observations of physical and physiological parameters of different plant species are performed to assess the impact of stress from environmental change [7]. Remote non-contact measurement of surface temperatures can be used to study the effects of global warming and droughts on ecosystems, as well as for various ecological studies [8].

Infrared radiometry is used to remotely measure the temperature on the studied surfaces. After detecting the changes, they are visualized and recorded for further analysis [9-17].

From a practical point of view, it is important to study to what angles and distances it is appropriate to perform radiometric studies in a real situation.

[1] Hristo Hristov is with the Faculty of Telecommunications at Technical University of Sofia, 8 Kl. Ohridski Blvd, Sofia 1000, Bulgaria, E-mail: hristoveu@gmail.com

[2] Kalin Dimitrov is with the Faculty of Telecommunications at Technical University of Sofia, 8 Kl. Ohridski Blvd, Sofia 1000, Bulgaria, E-mail: kld@tu-sofia.bg

II. THEORY

When performing radiometric studies in the infrared spectrum, we are always based on Planck's law of the emission of an ideal black body

$$M_{\lambda,\, black\, b.}(C) = \frac{c_1}{\lambda^5}\left(e^{\left(\frac{c_2}{\lambda T}\right)} - 1\right) , \qquad (1)$$

where M_λ is the spectral density of the radiation energy output, λ is the wavelength, T is the temperature, and

$c_1 = 2\pi c^2 h = 3{,}74.10^{-16}\, Wm^2$,

$c_2 = c\frac{h}{k_\delta} = 1{,}44.10^{-2}\, mK$.

All real bodies have their own radiant power, which is different from that of the ideal black body, and to be able to compare them, the radiation coefficient has been introduced

$$M_\lambda(\lambda, T) = \varepsilon(\lambda, T) M_{black\, b.}(\lambda, T) \ . \qquad (2)$$

In a real radiometric system for temperature measurements, there are energy interactions of the radiation with the atmospheric substance located between the studied object and the radiometer. Dispersion, absorption, as well as the thermal radiation of the atmosphere itself have an impact. Radiation from independent external sources or those resulting from repeated scattering can also enter the system. They propagate in different directions and those that coincide in direction with the radiation from the object under study are summed. Therefore, when describing energy transformations in a system, all influencing factors must be considered [9,19]. In our study, we focus on the flow coming from the object into the aperture of the radiometer.

In practice, when performing thermographic measurements, often the distance from the object to the radiometer is small enough and this makes the atmospheric channel uniform. Assuming that the object emits isotropic radiation, we will make measurements in the frequency range (8-12μm). The experimental setup is shown in Fig. 1.

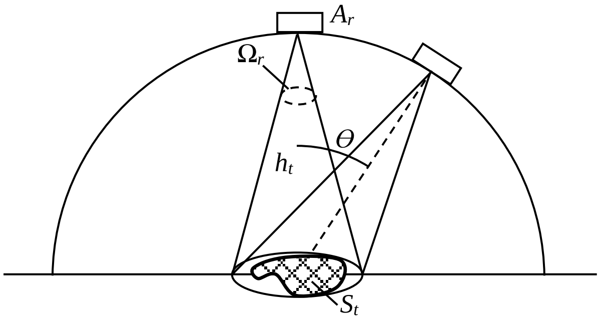

Fig. 1. Experimental setup

The expression

$$\Phi_{target} = A_r \Omega_r \tau_r \left\{ \varepsilon_t e^{-(\alpha^{(s)}+\alpha^{(a)})Z} F(T_t; \lambda_1, \lambda_2) \right\} , \quad (3)$$

where

$$F(T_t; \lambda_1, \lambda_2) = \int_{\lambda_1}^{\lambda_2} L_{\lambda, black\ b.}(\lambda, T) d\lambda \quad (4)$$

gives us the heat flux that reaches the aperture of the radiometer from the object, positioning it so that the axis of the angle of observation is perpendicular to the plane in which the object is located and falls into the geometric centre of the studied plane object [18].

It is often difficult in practice to create ideal conditions for non-contact remote temperature measurements. It is not always possible to observe the object of study perpendicularly, for example. Let us have a circular planar object with area S_target = 5m^2. We will monitor how the power of the heat flux from the object, which enters the aperture of the radiometer at different temperatures and viewing angles, as well as at different distances, changes. For this purpose, we will make ten series of calculations depending on the angle of observation, which we will change from zero to 90 degrees every ten degrees. For each series we will calculate the flow from the object at three different surface temperatures and we will change the distance between the radiometer and the object of observation from 3m to 7.5m with a step of 0.5m. This experimental setup could be used for practical observations in the infrared spectrum of field plantations, parts of experimental fields or forests for early detection of various types of stress, localization of diseases, infections, monitoring the spread of invasive species or results of human activity.

III. Numerical Investigation

For the purposes of the research, we choose the following parameters: [18, 20, 21]:
T_{t1}=303K; T_{t2}=293K; T_{t3}=283K; λ_1=8μm; λ_2=12μm; ε_t=0,98; ε_{scene}=0,8; $\alpha^{(s)}$=0,03km^{-1}; $\alpha^{(a)}$=0,4km^{-1}; $\Omega_r = 7{,}3.10^{-1}$; $\tau_r = 1$; $A_r = 8.10^{-5} m^2$

Table 1

Values of the heat flow entering the radiometer aperture from an object with surface area S_target=5 m^2 when the measurement distance is changed from 3 m to 7,5 m, trough 0,5 m for three different temperatures and perpendicular observation.

No	h target [m]	Φ_{target} [W], T=303K	Φ_{target} [W], T=293K	Φ_{target} [W], T=283K
1	3	0,001637295	0,001395587	0,001177082
2	3,5	0,001202652	0,001025109	0,000864609
3	4	0,000920582	0,00078468	0,000661824
4	4,5	0,000727217	0,000619861	0,00052281
5	5	0,000588919	0,000501979	0,000423385
6	5,5	0,000486606	0,00041477	0,00034983
7	6	0,000408796	0,000348447	0,000293891
8	6,5	0,000348248	0,000296838	0,000250362
9	7	0,000300211	0,000255892	0,000215827
10	7,5	0,000261461	0,000222862	0,000187969

Table 2

Values of the heat flow entering the radiometer aperture from an object with surface area $S_{target} = 5\ m^2$ when the measurement distance is changed from 3 m to 7,5 m, trough 0,5 m for three different temperatures and angle of observation 40 degrees.

No	h target [m]	Φ_{target} [W], T=303K	Φ_{target} [W], T=293K	Φ_{target} [W], T=283K
1	3	0,00213746	0,001821915	0,001536661
2	3,5	0,001570041	0,001338262	0,001128733
3	4	0,001201804	0,001024387	0,000864
4	4,5	0,00094937	0,000809218	0,00068252
5	5	0,000768824	0,000655326	0,000552722
6	5,5	0,000635255	0,000541475	0,000456697
7	6	0,000533676	0,000454892	0,00038367
8	6,5	0,000454632	0,000387517	0,000326844
9	7	0,00039192	0,000334062	0,000281759
10	7,5	0,000341333	0,000290943	0,00024539

TABLE 3

VALUES OF THE HEAT FLOW ENTERING THE RADIOMETER APERTURE FROM AN OBJECT WITH SURFACE AREA $S_{target} = 5\,m^2$ WHEN THE MEASUREMENT DISTANCE IS CHANGED FROM 3 M TO 7,5 M, TROUGH 0,5 M FOR THREE DIFFERENT TEMPERATURES AND ANGLE OF OBSERVATION 70 DEGREES.

No	h target [m]	Φ_{target} [W], T=303K	Φ_{target} [W], T=293K	Φ_{target} [W], T=283K
1	3	0,000731011	0,000623095	0,000525538
2	3,5	0,000536954	0,000457686	0,000386027
3	4	0,000411017	0,00035034	0,000295488
4	4,5	0,000324684	0,000276752	0,000233422
5	5	0,000262938	0,000224121	0,000189031
6	5,5	0,000217257	0,000185184	0,00015619
7	6	0,000182517	0,000155573	0,000131215
8	6,5	0,000155484	0,000132531	0,000111781
9	7	0,000134037	0,000114249	9,63615E-05
10	7,5	0,000116736	9,95025E-05	8,39235E-05

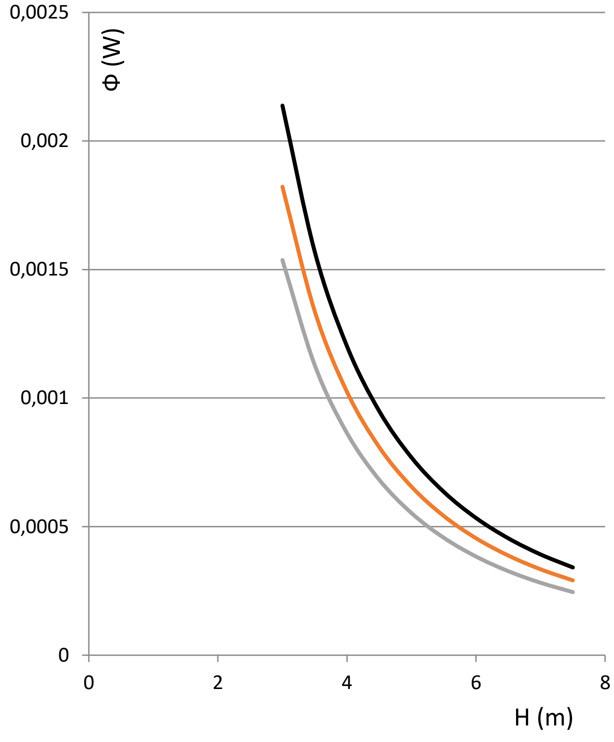

Fig 2. The change of the heat flow entering the radiometer aperture from an object with surface area $S_{target} = 5\,m^2$ when the measurement distance is changed from 3 m to 7,5 m, trough 0,5 m for three different temperatures and perpendicular observation. The black line shows the heat flux from the object, which enters the aperture of the radiometer at a temperature of 303K. The orange line is at a temperature of 293K and the gray line is at a temperature of 283K.

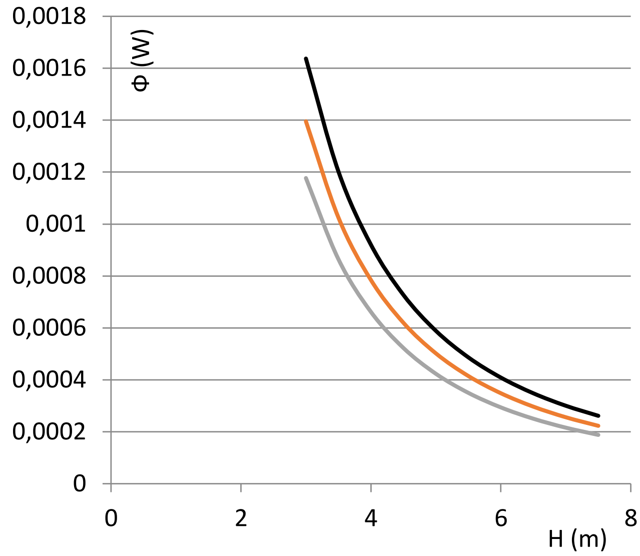

Fig.3. The change of the heat flow entering the radiometer aperture from an object with surface area $S_{target} = 5\,m^2$ when the measurement distance is changed from 3 m to 7,5 m, trough 0,5 m for three different temperatures and angle of observation 40 degrees. The black line shows the heat flux from the object, which enters the aperture of the radiometer at a temperature of 303K. The orange line is at a temperature of 293K and the gray line is at a temperature of 283K.

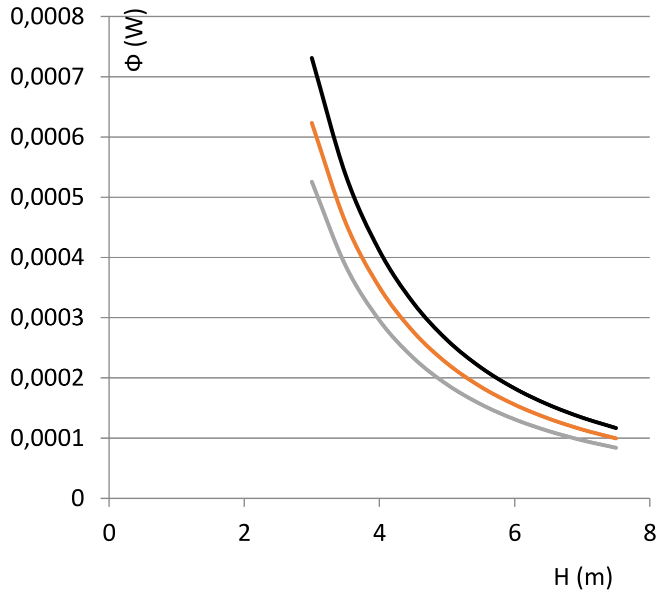

Fig. 4. The change of the heat flow entering the radiometer aperture from an object with surface area $S_{target} = 5\,m^2$ when the measurement distance is changed from 3 m to 7,5 m, trough 0,5 m for three different temperatures and angle of observation 70 degrees. The black line shows the heat flux from the object, which enters the aperture of the radiometer at a temperature of 303K. The orange line is at a temperature of 293K and the gray line is at a temperature of 283K.

The diagram with a family of graphs shown in Fig. 2 is corresponding to the data in Table 1. The study continues as with each subsequent series of calculations the angle of observation of the object with the radiometer increases by 10 degrees. We will now show the data at a 40-degree viewing angle. Numerical data are shown in Table 2.

The values showing the power of the flux entering the aperture of the radiometer decrease with the increasing viewing angle.

Fig. 3 shows a family of graphs corresponding to the results in Table 2.

Here are the results of the calculations at a 70-degree viewing angle. Numerical data are shown in Table 3.

It can be seen that the power of the flow entering the aperture of the radiometer continues to decrease with the increasing viewing angle.

Fig. 4 shows a family of graphs corresponding to the results in Table 3.

CONCLUSION

As the distance increases, the power of the current entering the aperture of the radiometer decreases. This makes it possible to register or increase the share of parasitic power from other sources and to cause or increase losses in the system. In a real situation, with increasing the angle of observation of the object, the incoming power decreases by law close to cosine, and at an angle of 40 degrees the values of the flow from the object decrease by about a quarter, and in the presence of other factors much more. The results of the study show that measurements in the infrared spectrum should be made from shorter distances and, if possible, the angle of observation should be perpendicular to the plane of the object or close to 90 degrees.

ACKNOWLEDGEMENT

We would like to thank the Research and Development Sector at the Technical University of Sofia for the financial support.

We would like to express our sincere gratitude to the Faculty of Telecommunications at the Technical University of Sofia for providing the laboratory base.

REFERENCES

[1] M. Wisniewski, M. Fuller, *Ice nucleation and deep supercooling in plants: new insights using infrared thermography*, Springer, 1999.

[2] M. Stoll, H.G. Jones, „Thermal imaging as a viable tool for monitoring plant stress“, Journal international des sciences de la vigne et du vin, vol. 41, no.2, pp.77-84, 2007.

[3] I. Romm, B. Cukurel, “Quantitative image fusion in infrared radiometry”, IOP, Measurement Science and Technology, vol. 29, no. 5, 2018.

[4] I. Kranner, G. Kastberger, M. Hartbauer, H. W. Pritchard, „Noninvasive diagnosis of seed viability using infrared thermography“, Proceedings of the National Academy of Sciences, vol. 107, no.8, pp. 3912–3917, 2010.

[5] M. Lindenthal, U. Steiner, H.W. Dehne, E.C. Oerke, “Effect of downy mildew development on transpiration of cucumber leaves visualized by digital infrared thermography”, Phytopathology, vol. 95, no. 3, pp.233-40, 2005.

[6] J.M. Costa, O.M. Grant, M.M. Chaves, „Thermography to explore plant–environment interactions“, Journal of Experimental Botany, vol.64, no.13, pp. 3937–3949, 2013.

[7] O.M. Grant, L. Tronina, H.G. Jones and M. Manuela Chaves, „Exploring thermal imaging variables for the detection of stress responses in grapevine under different irrigation regimes”, Journal of Experimental Botany, vol.58, no.4, pp.815–825, 2007.

[8] C. Still, R. Powell, D. Aubrecht, Y. Kim, B. Helliker, D. Roberts, A. D. Richardson, M. Goulden, „Thermal imaging in plant and ecosystem ecology: applications and challenges“, Ecosphere, vol.10, no.6, pp.e02768, 2019.

[9] M. Schlessinger, *Infrared Technology Fundamentals*, CRC Press, 1994.

[10] J. Miller, *Principles of Infrared Technology: A Practical Guide to the State of the Art*, Springer Science & Business Media, 2012.

[11] M. Diakides, J. Bronzino, D. Peterson, *Medical Infrared Imaging: Principles and Practices*, CRC Press, 2012.

[12] G. Zibordi, C. Donlon, A. Parr, *Optical Radiometry for Ocean Climate Measurements*, Academic Press, 2014.

[13] Z. Zhang, B. Tsai, G. Machin, *Radiometric Temperature Measurements: II. Applications*, Academic Press, 2009.

[14] W. Wolfe, *Introduction to Radiometry*, SPIE Press, 1998.

[15] N. Christoff, N. Bardarov, A. Manolova, K. Tonchev, "Feature Extraction and Automatic Detection of Wooden Vessels from Raster Images," 2020 XXIX International Scientific Conference Electronics (ET), pp.1-4, 2020.

[16] G. T. Nikolov, B. T. Ganev, M. B. Marinov and V. T. Galabov, "Comparative Analysis of Sensors for Soil Moisture Measurement", 2021 XXX International Scientific Conference Electronics (ET), pp.1-5, 2021.

[17] G. Popov, "Optimization of Communication Protocols for Data Transfer in Highly Noisy Environments", 2019 International Conference on Creative Business for Smart and Sustainable Growth (CREBUS), pp. 1-4, 2019.

[18] E. Ferdinandov, *Basics of optoelectronics*, Technika, 1993 (in Bulgarian).

[19] J.M. Palmer, B.G. Grant, *The Art of Radiometry*, SPIE, 2009.

[20] A. López, F.D. Molina-Aiz, D.L. Valera, A. Pena, „Determining the emissivity of the leaves of nine horticultural crops by means of infrared thermography”, Elsevier, Scientia Horticulturae, vol.137, pp.49–58, 2012.

[21] C. Chen, “Determining the Leaf Emissivity of Three Crops by Infrared Thermometry”, Sensors (Basel), vol.15, no.5, 2015.